



Analytical springback assessment and compensation in 3D multi-point flexible stretch bending forming

Ce Liang¹ · Yadan Luo^{1,2} · Jicai Liang^{2,3} · Yi Li¹

Received: 1 November 2022 / Accepted: 23 July 2023 / Published online: 13 September 2023
© The Author(s), under exclusive licence to Springer-Verlag London Ltd., part of Springer Nature 2023

Abstract

Due to the discrete die of multi-point stretch bending, there are contact zone and non-contact zone on the profile, which makes the springback phenomenon more complicated. In this paper, considering that the neutral layer will shift due to the application of pre-stretching and post-stretching, an analytical model of the relationship between springback error and stress is established. Under the different bending radius, the maximum springback error obtained by theoretical calculation is 6.9%, while the average springback error of the traditional springback model is 10.5%, which means that the springback prediction model proposed in this paper is more reliable. Multi-point stretch bending has been unanimously recognized by everyone because of its adjustable die surface. In this paper, the secant method is used to calculate the springback compensation factor, so that the springback error of the profile is within the allowable error range of the production under the limited numbers of springback compensation.

Keywords Hollow rectangular profile · Multi-point stretch bending · Springback model · Springback compensation

1 Introduction

Multi-point stretch bending forming, which separates the traditional integral die into a series of independently adjustable die, has been unanimously recognized in the industrial production because of its adjustable die surface [1–3]. Due to the discrete dies, which are contact with the profile discontinuously, there are several contact zones and non-contact zones on the forming surface of the profile, leading to a certain impact on the forming accuracy and forming quality [4]. Additionally, after the clamp is unloaded, the presence of residual stress will inevitably lead to springback. Springback is the main factor affecting the accuracy of metal bending, and it is also one of the research hotspots in the field of bending [5–8]. Obviously, different process

parameters will affect the springback of the profile [9]. In the process of multi-point stretch bending, the pre-stretching and post-stretching have a great impact on the springback of the profile. Within the appropriate range, the use of appropriate pre-stretching and post-stretching can effectively reduce the springback of the profile.

For the problem of springback, relevant scholars all over the world have carried out a lot of further research and discussion, from theoretical analysis to numerical simulation, from springback prediction to comparative experiments, and so on. J. Ma et al. [10] comprehensively considered the influencing factors such as material properties, geometry, and process parameters, considered the distribution of the moment along the entire contour during bending, and innovatively developed a full moment (FM) analysis model for springback evaluation. By comparing experiments, numerical simulation, and analytical calculation, it is demonstrated that the developed FM model provides accurate and effective springback assessment. Considering the Young's modulus (E), neutral layer (D_e), and wall thickness (t), Mei Zhan et al. [11] established an analytic elastic-plastic tube bending springback model based on the static equilibrium condition, which greatly reduced the springback prediction error.

As we all know, springback is unavoidable. In order to form a part with qualified shape, we must take certain

✉ Yi Li
liyijlu@126.com

¹ Key Laboratory of Automobile Materials, Ministry of Education, and College of Materials Science and Engineering, Jilin University, Changchun 130025, China

² Roll Forging Research Institute, Jilin University, Changchun 130025, Jilin, China

³ Chongqing Research Institute, Jilin University, Chongqing 401123, China

measures to make the shape of the parts after springback consistent with the curvature of the target part as much as possible. In the process of multi-point stretch bending, we can continuously adjust the curvature of the forming die to form parts with qualified shape. Springback compensation is the optimal solution to solve this kind of problem [12]. At present, a large number of scholars all over the world have also made a lot of research in the field of springback compensation.

Yong Li et al. [13] combined the springback mechanism of the plate with the creep-aging behavior of materials for tool design in the creep age forming (CAF) process to manufacture both singly and varyingly curved products. Springback compensation curves that relate the objective shapes and springback compensated shapes by their curvature, stress, and strain states have been established, based on the numerical solution of springback behavior of CAF process. Qing-Fang Zhang et al. [14] used a combination method of theoretical analysis, numerical simulation, and forming experiments to propose the springback compensation and modification for doubly curved plate, that is, using interpolation processing and Bezier surface blending methods to describe the shape of die surface after springback compensation.

Compared with traditional stretch bending forming, multi-point stretch bending forming has the characteristics of contact zone and non-contact zone, which makes the springback problem more difficult to control. Therefore, how to effectively evaluate the springback phenomenon has become an urgent problem to be solved in the process of multi-point stretch bending. In this paper, an analytical model of the relationship between springback and stress is established. Using numerical simulation or strain gauge experiment, we can measure the stress and strain changes of the profile during the multi-point stretch bending process, so as to obtain the springback error of the profile. Through a large number of numerical simulations and comparative experiments, we confirm the reliability of the analytical model. The biggest advantage of multi-point stretch bending is that the die surface can be adjusted. In this paper, the secant method is used to calculate the springback compensation factor, which can improve the efficiency of springback iterative compensation,

so that the springback error of the profile is within the allowable error range of the production under the limited numbers of springback compensation.

2 Basic analysis of multi-point stretch bending forming

2.1 Basic assumptions

- (1) After the bending deformation, the section of the profile is flat and perpendicular to the tangent of the geometric center axis.
- (2) During the bending process, the radial stress and transverse stress of the profile are ignored, and only the axial stress is considered.

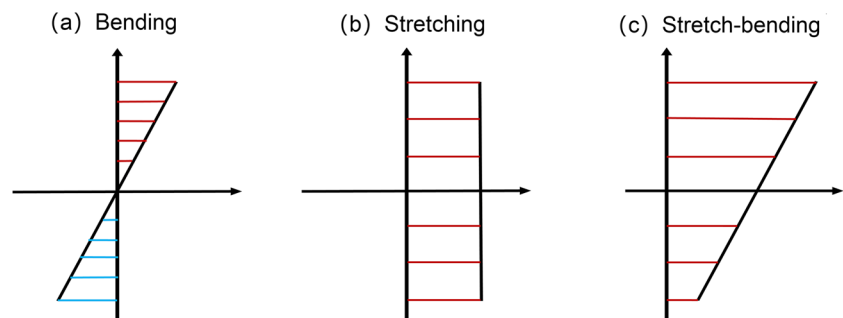
$$\begin{cases} \sigma_{ij} = 0 \ (i \neq j) \\ \varepsilon_{ij} = 0 \ (i \neq j) \\ \sigma_r = 0, \varepsilon_r = 0 \\ \sigma_\varphi = 0, \varepsilon_\varphi = 0 \end{cases} \quad (1)$$

- (C) The loading and unloading laws of the profile conform to the classical elastic-plastic theory during the bending process.
- (D) The cross-sectional distortion of the rectangular profile in the process of stretch bending is ignored.

2.2 Stress and strain analysis of multi-point stretch bending

As shown in Fig. 1, in the process of pure bending, the upper part of the neutral layer is subjected to tensile stress, showing a trend of elongation, and the lower part is subjected to compressive stress, showing a trend of shrinkage. During the stretch bending process, after applying a certain amount of pre-stretching and post-stretching, the neutral layer of the profile will gradually shift downward [15, 16]. When the amount of pre-stretching and post-stretching are large enough, the neutral layer of the profile will be offset from the lower bottom surface, resulting in a completely plastic tensile deformation inside the profile

Fig. 1 Stress distribution during stretch-bending



[17]. In the process of multi-point stretch bending in this paper, after the pre-stretching, bending and post-stretching, the profile presents complete plastic tensile deformation, and the section stress distribution results are shown in Fig. 2. In the bending plane shown in Fig. 2, the bending radius of the geometric center layer of the profile is ρ ; after multi-point stretch bending, the bending radius of the strain neutral layer of is ρ_ϵ . From the basic assumptions, we can know that:

$$\epsilon = \frac{(\rho_\epsilon + z)d\theta - \rho_\epsilon d\theta}{\rho_\epsilon d\theta} \tag{2}$$

In the strain neutral layer coordinate system XOZ , the expression of strain in multi-point stretch bending is as follows:

$$\epsilon = \frac{Z}{\rho_\epsilon} \tag{3}$$

where Z is the distance from the desired point to the neutral layer. It can be known from the coordinate conversion relationship that in the coordinate system of the geometric center layer, $Z = u + \rho - \rho_\epsilon$, so the strain in multi-point stretch bending can be expressed as:

$$\epsilon = \frac{u + \rho - \rho_\epsilon}{\rho_\epsilon} \left(-\frac{H}{2} \leq u \leq \frac{H}{2} \right) \tag{4}$$

In this paper, the profile used in multi-point stretch bending is 6005A aluminum alloy, and the relationship between its stress and strain satisfies the bilinear isotropic strengthening material model, that is:

$$\begin{cases} \sigma = E\epsilon & (\epsilon \leq \epsilon_s) \\ \sigma = \sigma_s + (\epsilon - \epsilon_s)D & (\epsilon > \epsilon_s) \end{cases} \tag{5}$$

where E is the Young’s modulus, D is the plastic modulus, σ_s is the yield stress, and ϵ_s is the yield strain.

In this paper, the profile is a completely plastic tensile deformation, so the stress relationship between the upper and lower surfaces is as follows:

$$\begin{cases} \sigma_A = \sigma_s + \left(\frac{\frac{H}{2} + \rho - \rho_\epsilon}{\rho_\epsilon} - \epsilon_s \right) D \\ \sigma_B = \sigma_s + \left(\frac{-\frac{H}{2} + \rho - \rho_\epsilon}{\rho_\epsilon} - \epsilon_s \right) D \end{cases} \tag{6}$$

From formula (6), it can be deduced that:

$$\sigma_A - \sigma_B = \frac{DH}{\rho_\epsilon} \tag{7}$$

2.3 Springback analysis of multi-point stretch bending

After multi-point stretch bending deformation, the balance relationship between internal force and external load is as follows:

$$\int_0^A \sigma \cdot u dA = M \tag{8}$$

In this paper, the profile is fully plastic tensile deformation, and substituting formula (5) into formula (8), it can be obtained that:

$$M = \int_{-\frac{H}{2}}^{\frac{H}{2}} \left[\sigma_s + \left(\frac{u + \rho - \rho_\epsilon}{\rho_\epsilon} - \epsilon_s \right) D \right] u \cdot B_{(u)} du \tag{9}$$

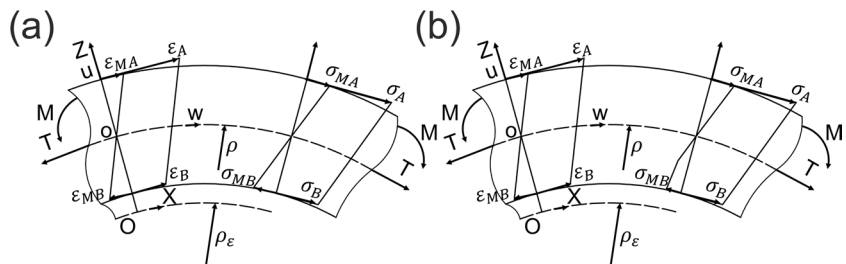
where $B_{(u)}$ is the width of each section, H is the section height of the rectangular profile, and A is the section area of the profile. Through formula (9), the analytical formula of the bending moment M can be obtained as:

$$M = \frac{DI_v}{\rho_\epsilon} \tag{10}$$

where $I_v = \int_0^A u^2 dA = \int_{-\frac{H}{2}}^{\frac{H}{2}} u^2 \cdot B_{(u)} du$. The profile used in this paper is a hollow rectangular profile, its width is B , its height is H , and its wall thickness is t , so,

$$I_v = \frac{BH^3}{12} - \frac{(B - 2t)(H - 2t)^3}{12} \tag{11}$$

Fig. 2 a Fully plastic tensile deformation under elastic bending. **b** Fully plastic tensile deformation under plastic bending



From formulas (7) to (10), the relationship between bending moment and stress can be obtained as:

$$M = \frac{\sigma_A - \sigma_B}{H} \cdot I_v \tag{12}$$

In the process of multi-point stretch bending, the profile will have a large internal stress. After the external load is removed, it will inevitably make the profile springback and affect the forming accuracy of the profile. The relationship between the curvature of the profile before and after the springback is as follows:

$$\Delta k = \frac{1}{R_e} - \frac{1}{R} = \frac{M_e}{EI_v} \tag{13}$$

In the process of multi-point stretch bending, the profile has the following relationship when the load is applied and the load is unloaded:

$$M + M_e = 0 \tag{14}$$

Therefore, by combining formulas (12)–(14), we can get:

$$R_e = \frac{REH}{EH - R(\sigma_A - \sigma_B)} \tag{15}$$

The commonly used evaluation methods for the springback phenomenon of stretch bending mainly include springback angle and springback gap [18, 19]. In this paper, the springback gap Δx is used to represent the springback error of the profile. As shown in Fig. 3, the springback curvature radius of the profile is R_e , and the die curvature radius is R . Therefore, the distance from the farthest lower surface of the profile to the center point is:

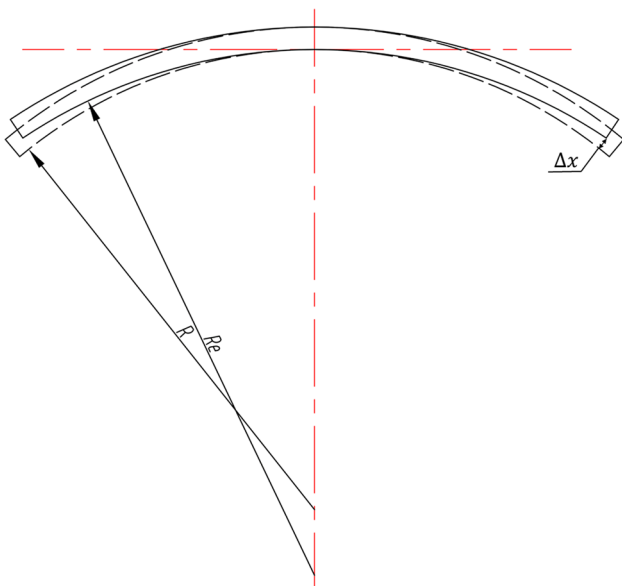


Fig. 3 Definition of springback gap

$$\begin{cases} X = R_e \sin\left(\frac{L}{2R_e}\right) \\ Y = R_e \left[1 - \cos\left(\frac{L}{2R_e}\right)\right] \end{cases} \tag{16}$$

Therefore, we can easily get formula (17) for calculating the springback gap of the profile after unloading:

$$\Delta x = \sqrt{X^2 + (R - Y)^2} - R \tag{17}$$

Using the finite element platform for numerical simulation or strain gauge for bridge connection test, the stress and strain on the upper and lower surfaces of the profile can be easily obtained. Substituting these known quantities into formulas (14)–(16), we can obtain the springback gap of the profile.

2.4 Springback compensation of multi-point stretch bending

Compared with the integral die forming, the most significant advantage of the multi-point stretch bending is that the die surface is adjustable, which greatly facilitates the iterative compensation of springback, so that the springback error of the profile is within the allowable error range of the production. The DA method is one of the most classic methods of springback compensation, as shown in Fig. 4:

$$C^{j+1} = C^j - \alpha(S^j - O) \tag{18}$$

where C^{j+1} and C^j are the die curvature after the $j + 1_{th}$ and j_{th} adjustment respectively, O is the target curvature, S^j is the curvature of the part obtained after the j_{th} adjustment, and α is the springback compensation factor.

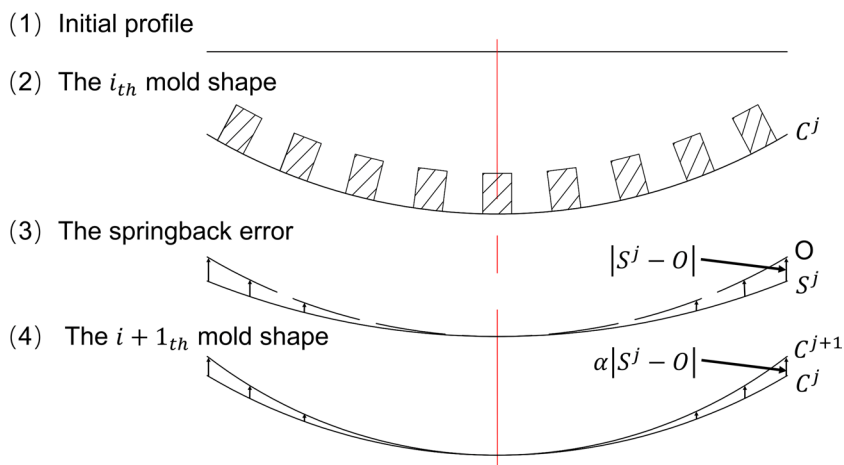
When $|S^j - O| < \varepsilon$, that is to say, the springback is within the allowable error range of the production. The die curvature C^j is the die curvature for forming the target part.

The springback compensation factor is mainly used to speed up the efficiency of the springback compensation, so that the die surface with the springback error within the allowable error range of the production can be obtained under less compensation times. In this paper, we use the secant method to establish the relationship between the springback compensation factor and the curvature of the profile:

$$\alpha^{i+1} = \alpha^i - (S^i - O) \frac{\alpha^i - \alpha^{i-1}}{S^{i-1} - S^i} \tag{19}$$

where α^{i+1} , α^i , and α^{i-1} are the springback compensation factors of the $i + 1_{th}$, i_{th} , and $i - 1_{th}$ times, respectively. The first two values of α can be given as $\alpha^0 = 0$ and $\alpha^1 = 0.8$, and all subsequent values of α^i can be iterated by

Fig. 4 Springback compensation steps of multi-point stretch bending

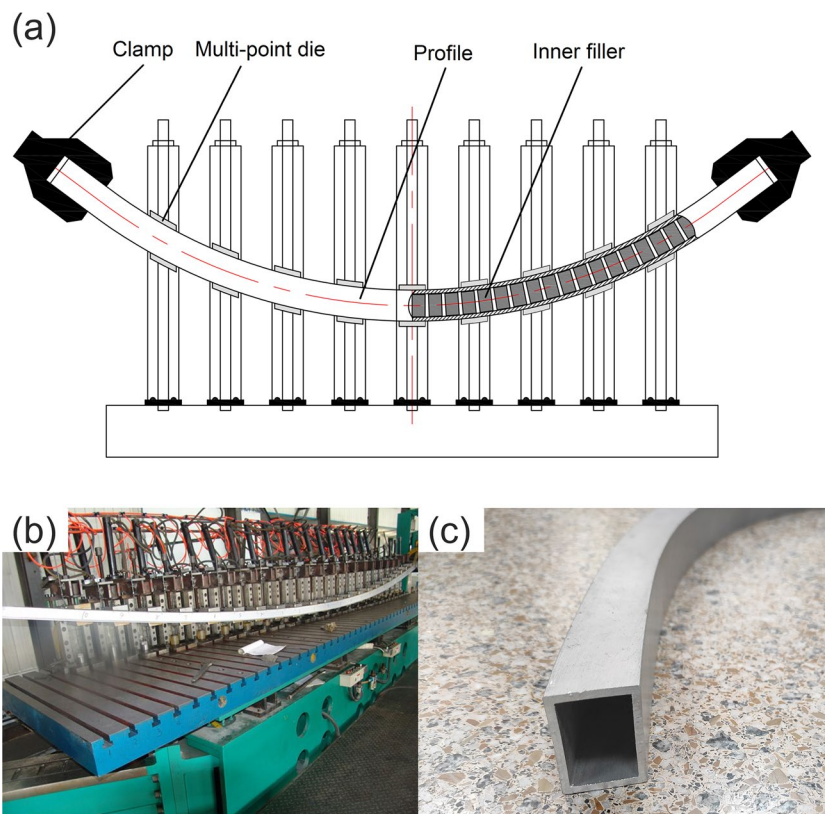


using formulas (17) and (18). When the springback error obtained under different iteration times is within the allowable error range of the production, we can consider that the springback iteration compensation is completed. The springback compensation factor is calculated by the secant method, when the springback error is large, the springback compensation factor we get is large, which can speed up the efficiency of springback compensation; when the springback error is small, the springback compensation factor we get is small, which can improve the accuracy of springback compensation.

2.5 The principle and finite element model of multi-point stretch bending

Multi-point stretch bending forming mainly through the following steps: pre-stretching, bending, post-stretching to form qualified parts. As shown in Fig. 5a, the multi-point stretch bending machine clamps the parison, and attaches the profile to the discrete die curvature according to the multi-point stretch bending forming steps, so that the profile is formed into the target shape. By adjusting the discrete die curvature, the die surface can be adjusted freely to form target part with different curvatures.

Fig. 5 a Schematic diagram of multi-point stretch bending. b Multi-point stretch bending machine (c) part



After the clamp is unloaded, the profile will springback due to the internal residual stress, which seriously affects the forming accuracy of the profile. As shown in Fig. 5b, in order to study the springback of hollow rectangular profile after unloading during the multi-point stretch bending process, a large number of experiments have been carried out using the multi-point stretch bending machine. Figure 5c shows the part formed by multi-point stretch bending. Comparing the forming curvature of these parts with the target curvature, the springback error of profile during the multi-point stretch bending process can be obtained.

In this paper, the ABAQUS/Explicit analysis module is used to perform a dynamic analysis of the stretch bending process, and the ABAQUS/standard analysis module is used to perform a static analysis of the springback process. The model is shown in Fig. 6. In order to reduce the time required for the simulation, the model can be simplified appropriately. The strength and hardness of clamps and dies are much greater than the profile, so they can be regarded as rigid body, and the meshing type is R3D4. The main research object is the hollow rectangular profile with a total length of 3000 mm. Therefore, it is necessary to precisely divide the profile mesh, and the meshing type is C3D8R. The interaction between the profile and the die is set to “hard contact,” and the friction coefficient is 0.1. The contact between the clamp and the profile is a “Tie” constraint, the main surface is the inner surface of the clamp, and the slave surface is the outer surface of the profile. The boundary conditions are defined according to the clamp displacement trajectory to make the simulation process consistent with the actual operating conditions.

3 Results and discussion

3.1 The stress analysis of multi-point stretch bending

In the process of multi-point stretch bending, the springback is a common phenomenon, which is the accumulation of the error in the whole forming process. The springback phenomenon is related to many factors, such as the performance parameters and geometric parameters of the material, and

the process parameters used during processing, and so on. Therefore, in order to form parts with qualified springback error, it is necessary to study and analyze the springback phenomenon. The changes of internal stress and strain of the parts are the main reason for the various defects, and the springback error during unloading is no exception. Among them, the springback is mainly related to the residual springback bending moment remaining in the production during the processing, and the springback phenomenon will occur after the clamp is unloaded.

In this paper, we establish an analytical model of the relationship between springback and internal stress of the profile. Through the distribution of the stress and strain, we can intuitively analyze the size of the springback gap and understand the various relationship between the stress and the springback error. Using this analytical model combined with finite element numerical simulation, the deformation characteristics of the profile in the process of multi-point stretch bending are analyzed. Under the conditions of 1% pre-stretching, 1% post-stretching, and the bending radius $R = 5000$ mm, we obtained the stress distribution diagram as shown in Fig. 7a. Since the profile is symmetrical about the center plane during the multi-point stretch bending process, only-half of the profile is taken to show the deformation.

In the process of multi-point stretch bending, there are contact zone and non-contact zone on the profile, and there are certain differences in the force between the contact zone and the non-contact zone. Therefore, the stress and strain distribution of the profile is more complicated than that of the integral die stretch bending. In this paper, we can extract the stress distribution diagram of the upper and lower surfaces of the profile during the multi-point stretch bending process through the paths A and B shown in Fig. 7b.

Taking the center plane as the origin of the coordinate and the distance from the center plane as the X-axis on the paths A and B, the stress distribution on the upper and lower surfaces of the profile as shown in Fig. 8 is obtained. The stress difference between the upper and lower surfaces is small in the central area, and the stress difference is greater on both sides. For the lower surface area of the

Fig. 6 Finite element assembly drawing of multi-point stretch bending

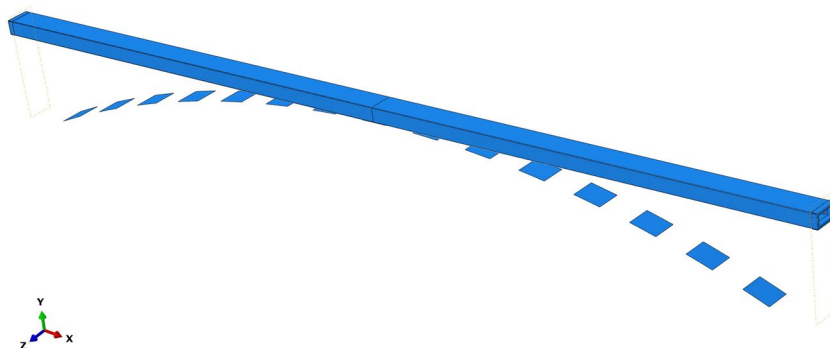


Fig. 7 **a** Stress distribution of finite element simulation. **b** The paths A and B

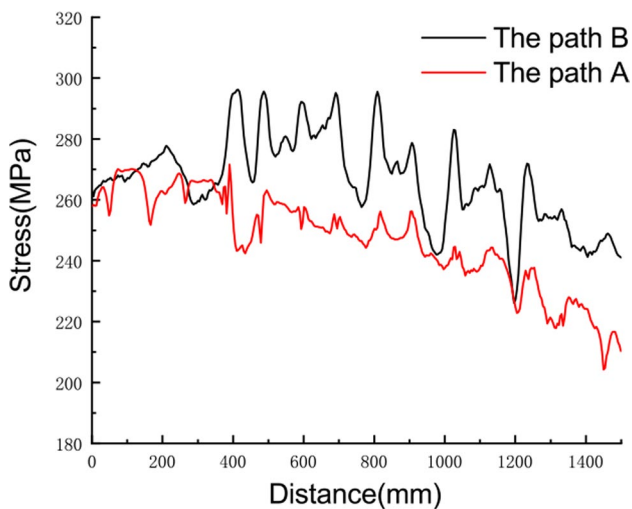
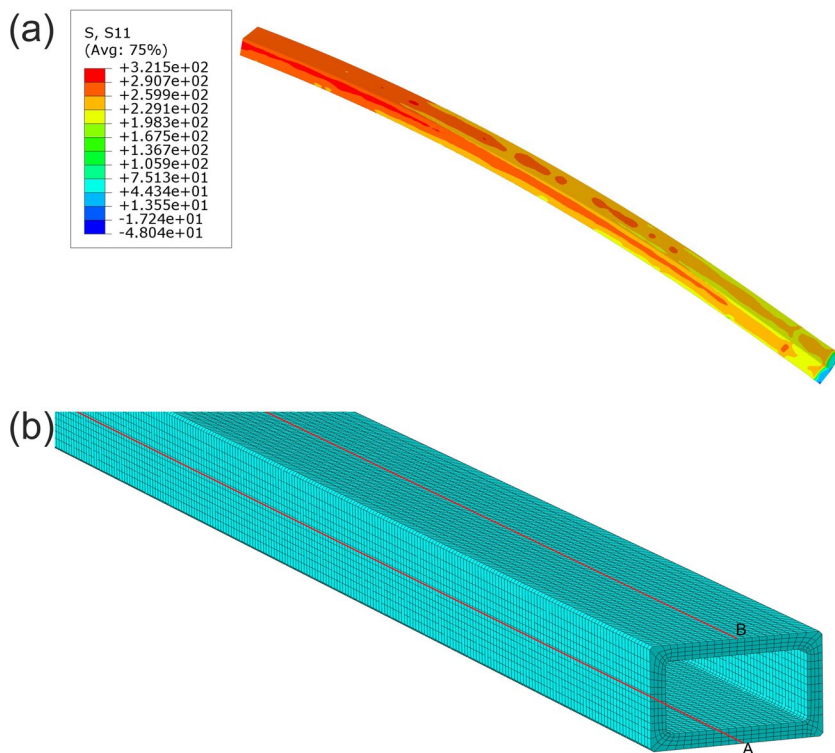


Fig. 8 Stress distribution along paths A and B

profile, the stress at the center is larger, and as the extraction area moves away from the center plane, the stress gradually begins to decrease, which means that the axial stress at the bottom of the profile reaches its maximum value near the center plane. For the upper surface area of the profile, the stress distribution is extremely uneven, which is significantly different from the stress distribution on the lower surface. This is mainly because the contact zone of

the lower surface area is in direct contact with the die and is supported by the die, but the contact zone of the upper surface is not in direct contact with the die, and the connection between the contact zone and the die is transmitted through the lower surface. Therefore, the distribution of stress on the lower surface has been changed, leading to a deviation in the distribution law of stress.

The distribution of the stress difference between the upper and lower surfaces of the profile is shown in Fig. 9. When the profile is closer to the center plane (less than 389 mm), the axial stress difference between the upper and lower surfaces is small; when the profile is farther away from the center plane (more than 389 mm), the stress difference between the upper and lower surfaces is large. The maximum difference between them is 52.836 MPa, which appears at 410.06 mm from the center plane. In the contact zone, the contact between the profile and die is surface contact. Due to the support of the die, the average stress difference between the upper and lower surfaces in the contact zone is usually greater than that in the non-contact zone. The boundary between the contact zone and the non-contact zone can be considered as line contact between the profile and die. Compared with the contact zone and the non-contact zone, the stress of the profile at this boundary changes abruptly, resulting in the stress difference between the upper and lower surfaces at this location is usually greater than that at both sides.

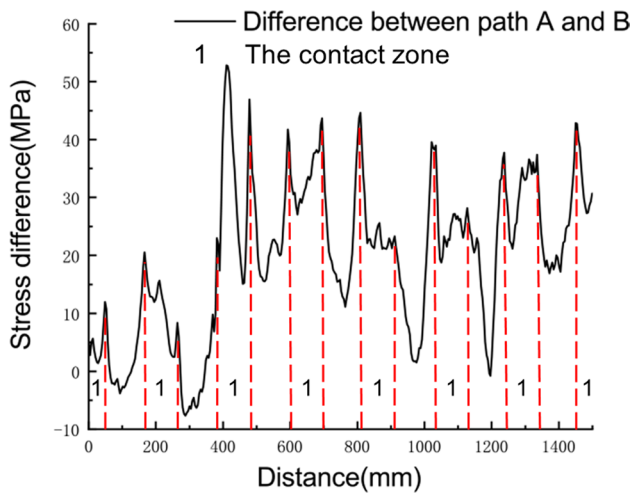


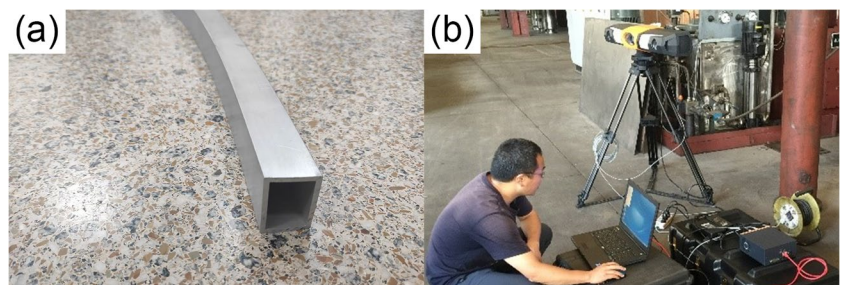
Fig. 9 Distribution of stress difference along paths A and B

3.2 Analysis of springback error in multi-point stretch bending

There is a close relationship between stress and springback. It is the influence of the springback bending moment caused by residual stress that makes the parts springback. In this paper, by establishing an analytical model of the relationship between stress and springback, we can predict the springback error of the different bending radius, which has a certain positive significance to study the springback phenomenon of the profile. The ABAQUS/standard analysis module is used to simulate the springback process of the profile in multi-point stretch bending. Through a large number of numerical simulations and multi-point stretch bending experiments, we can verify the accuracy of the springback analytical model in the process of multi-point stretch bending. As shown in Fig. 10a, the formed profile has good forming quality. We use the PRO CMM 3500 3D scanning system as shown in Fig. 10b to obtain the spatial coordinates of the profile surface, and compare the scanning surface with the die surface to obtain the springback error of the profile.

Figure 11 shows the springback error of the profile under different bending radius. When the bending radius is 4000 mm, the springback error obtained by theoretical calculation is 6.38

Fig. 10 a Formed profile. b PRO CMM 3500 3D scanning system



mm, and the springback error obtained by numerical simulation is 6.82 mm. The difference between them is large, reaching 6.9%. With the increase of bending radius, the difference between the numerical simulation and the theoretical calculation results gradually decreases. Under the different bending radius, the maximum springback error obtained by theoretical calculation is 6.9%, while the average springback error of the traditional springback model is 10.5%, which means that the springback prediction model proposed in this paper is more reliable. The springback error of the profile obtained by the experiment of the multi-point stretch bending machine is basically consistent with the springback error obtained by the theoretical calculation and numerical simulation. In general, the trend of springback error obtained by theoretical calculation, numerical simulation, and experiment is consistent, and the correlation is good, which can basically verify the accuracy of the springback analytical model.

3.3 Application of springback compensation method

In the process of multi-point stretch bending, the springback of the profile will inevitably occur after the clamp is

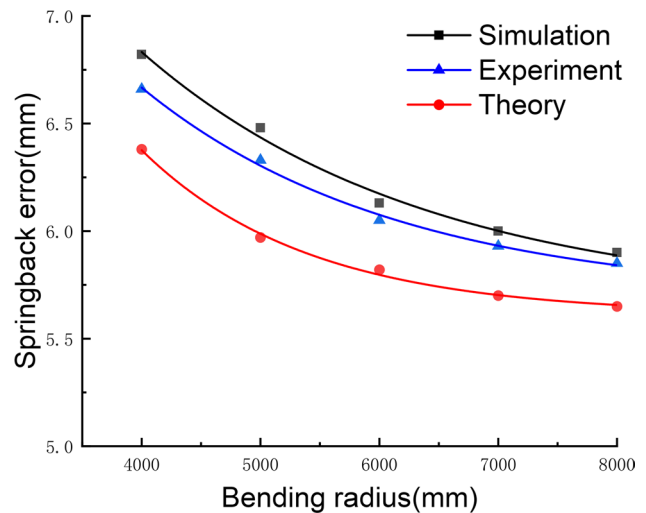


Fig. 11 Springback error diagram of the profile under different bending radius

unloaded, resulting in a certain error between the forming curvature and the target curvature. In order to form profile with qualified shape, it is necessary to make appropriate springback compensation for the die. In this paper, the DA method is used to perform springback iterative compensation on the die surface, and the springback compensation factor is calculated by the secant method. The curvature obtained after each iteration compensation is compared with the target curvature to determine whether the industrial requirements are satisfied or not. If not, the iterative compensation is continued until the springback error is within the allowable error range of the production. When the springback error is large, a larger springback compensation factor can be obtained by the secant method, thereby speeding up the efficiency of springback compensation; when the springback error is small, a smaller springback compensation factor can be obtained by the secant method, thereby improving the precision of springback compensation. Taking the center plane as the coordinate origin, and the distance from the profile to the center plane as the X -axis, we measured the springback error between the shape of the profile and the target curvature, and the results are shown in Fig. 12. When springback compensation is not used, the springback error between the profile curvature and the target curvature is large, and the maximum value is 6.48 mm. After multiple springback compensation, the springback error between the profile curvature and the target curvature is significantly reduced, the maximum springback error is reduced from 6.48 to 1.16 mm, and the maximum springback error is reduced by 82%. After several times of springback iterative compensation, the maximum springback error of the profile is within the allowable error range of the production, which confirms the feasibility of springback compensation.

4 Conclusion

- (1) In this paper, an analytical model of the relationship between springback error and stress is established. The stress difference between the upper and lower surfaces of the profile can be measured by numerical simulation on the finite element platform or the strain gauge experiment, so that the springback error of the profile in the process of multi-point stretch bending can be obtained.
- (2) Comparing the theoretical calculation, numerical simulation, and experimental results, the springback error of the profile between them has the same trend, and the relative deviation is small, which confirms the accuracy of the multi-point stretch bending springback analytical model.
- (3) Multi-point stretch bending is widely recognized because of its adjustable die surface. In this paper, we

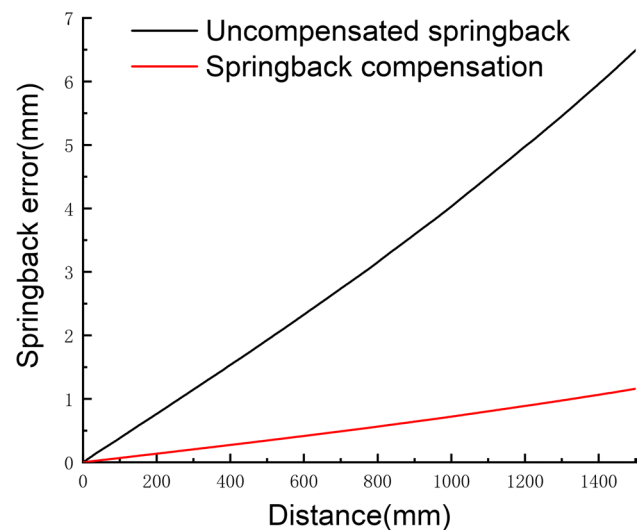


Fig. 12 Distribution of springback error of the profile when bending radius $R = 5000$ mm

use the secant method to calculate the springback compensation factor, so that the springback error of the profile is within the allowable error range of the production under the limited numbers of springback compensation.

Author contribution C. Liang: data curation, investigation, writing — review and editing. Y. Luo: methodology, investigation, writing — original draft. J. Liang: funding acquisition, project administration, methodology. Y. Li: conceptualization, data curation, formal analysis, methodology, investigation, writing — original draft.

Funding This work was funded by the Project of Jilin Provincial Scientific and Technological Department (20220201048GX).

Data availability At this time the processed/raw data required to regenerate the outcomes of the present study cannot be shared as these data are also a part of ongoing research.

Code availability Not applicable.

Declarations

Conflict of interest The authors declare no competing interests.

References

1. Cai ZY, Li MZ (2001) Optimum path forming technique for sheet metal and its realization in multi-point forming. *J Mater Process Technol* 110:136–141. [https://doi.org/10.1016/s0924-0136\(00\)00837-2](https://doi.org/10.1016/s0924-0136(00)00837-2)
2. Li MZ, Cai ZY, Sui Z, Yan QG (2002) Multi-point forming technology for sheet metal. *J Mater Process Technol* 129:333–338. [https://doi.org/10.1016/s0924-0136\(02\)00685-4](https://doi.org/10.1016/s0924-0136(02)00685-4)

3. Liang J, Chen C, Li Y, Liang C (2020) Effect of roller dies on springback law of profile for flexible 3D multi-point stretch bending. *Int J Adv Manuf Technol* 108:3765–3777. <https://doi.org/10.1007/s00170-020-05655-6>
4. Chen C, Liang J, Li Y, Liang C (2021) Effect of discrete roller dies on the contour accuracy of profiles in multi-point flexible stretch-bending forming. *Int J Adv Manuf Technol* 113:1959–1971. <https://doi.org/10.1007/s00170-021-06727-x>
5. Chatti S, Hermi N (2011) The effect of non-linear recovery on springback prediction. *Comput Struct* 89:1367–1377. <https://doi.org/10.1016/j.compstruc.2011.03.010>
6. Zhan M, Huang T, Zhang PP, Yang H (2014) Variation of Young's modulus of high-strength TA18 tubes and its effects on forming quality of tubes by numerical control bending. *Mater Des* 53:809–815. <https://doi.org/10.1016/j.matdes.2013.07.070>
7. Ma J, Li H, Fu MW (2021) Modelling of springback in tube bending: a generalized analytical approach. *Int J Mech Sci* 204:106516. <https://doi.org/10.1016/j.ijmecsci.2021.106516>
8. Cui X, Du Z, Xiao A, Yan Z, Qiu D, Yu H, Chen B (2021) Electromagnetic partitioning forming and springback control in the fabrication of curved parts. *J Mater Process Technol* 288:116889. <https://doi.org/10.1016/j.jmatprotec.2020.116889>
9. Chen C, Liang J, Li Y, Liang C, Jin W (2021) Springback analysis of flexible stretch bending of multi-point roller dies process for Y-profile under different process parameters. *Metals* 11(4):646. <https://doi.org/10.3390/met11040646>
10. Ma J, Welo T (2021) Analytical springback assessment in flexible stretch bending of complex shapes. *Int J Mach Tool Manu* 160:103653. <https://doi.org/10.1016/j.ijmachtools.2020.103653>
11. Zhan M, Wang Y, Yang H, Long H (2016) An analytic model for tube bending springback considering different parameter variations of Ti-alloy tubes. *J Mater Process Technol* 236:123–137. <https://doi.org/10.1016/j.jmatprotec.2016.05.008>
12. Li Y, Liang Z, Zhang Z, Zou T, Li D, Ding S, Xiao H, Shi L (2019) An analytical model for rapid prediction and compensation of springback for chain-die forming of an AHSS U-channel. *Int J Mech Sci* 159:195–212. <https://doi.org/10.1016/j.ijmecsci.2019.05.046>
13. Li Y, Rong Q, Shi Z, Sun X, Meng L, Lin J (2019) An accelerated springback compensation method for creep age forming. *Int J Adv Manuf Technol* 102:121–134. <https://doi.org/10.1007/s00170-018-3175-3>
14. Zhang QF, Cai ZY, Zhang Y, Li MZ (2013) Springback compensation method for doubly curved plate in multi-point forming. *Mater Des* 47:377–385. <https://doi.org/10.1016/j.matdes.2012.12.005>
15. Li H, Ma J, Liu BY, Gu RJ, Li GJ (2018) An insight into neutral layer shifting in tube bending. *Int J Mach Tool Manu* 126:51–70. <https://doi.org/10.1016/j.ijmachtools.2017.11.013>
16. Wang A, Xue H, Saud S, Yang Y, Wei Y (2019) Improvement of springback prediction accuracy for Z-section profiles in four-roll bending process considering neutral layer shift. *J Manuf Process* 48:218–227. <https://doi.org/10.1016/j.jmapro.2019.11.008>
17. Zhai R, Ding X, Yu S, Wang C (2018) Stretch bending and springback of profile in the loading method of prebending and tension. *Int J Mech Sci* 144:746–764. <https://doi.org/10.1016/j.ijmecsci.2018.06.028>
18. Zhu YX, Liu YL, Yang H, Li HP (2013) Improvement of the accuracy and the computational efficiency of the springback prediction model for the rotary-draw bending of rectangular H96 tube. *Int J Mech Sci* 66:224–232. <https://doi.org/10.1016/j.ijmecsci.2012.11.012>
19. Xue X, Liao J, Vincze G, Gracio JJ (2015) Modelling of mandrel rotary draw bending for accurate twist springback prediction of an asymmetric thin-walled tube. *J Mater Process Technol* 216:405–417. <https://doi.org/10.1016/j.jmatprotec.2014.10.007>

Publisher's note Springer Nature remains neutral with regard to jurisdictional claims in published maps and institutional affiliations.

Springer Nature or its licensor (e.g. a society or other partner) holds exclusive rights to this article under a publishing agreement with the author(s) or other rightsholder(s); author self-archiving of the accepted manuscript version of this article is solely governed by the terms of such publishing agreement and applicable law.